Research Square

Preprints are preliminary reports that have not undergone peer review.
They should not be considered conclusive, used to inform clinical practice,
or referenced by the media as validated information.

Development and Microstructural Investigation of Ni– Mo–FeCrAl Modified 40H Steel for Furnace Roller Applications

Aigerim Zhalel
Abylkas Saginov Karaganda Technical University
Ardak Dostayeva
Abylkas Saginov Karaganda Technical University
Anna Bogdanova
aneta.2011@mail.ru
Abylkas Saginov Karaganda Technical University
Yerkebulan Nartbay
Abylkas Saginov Karaganda Technical University

Article

Keywords: 40H steel, complex alloying, Ni-Mo modification, FeCrAl, heat treatment, SEM/BSE analysis, local EDS assessment, furnace roller applications

Posted Date: November 16th, 2026

DOI: https://doi.org/10.21203/rs.3.rs-11404091/v1

License: This work is licensed under a Creative Commons Attribution 4.0 International License.
Read Full License

Additional Declarations: No competing interests reported.

Development and Microstructural Investigation of Ni–Mo–FeCrAl Modified 40H Steel for Furnace Roller Applications

Aigerim Zhalel[1], Ardak Dostayeva[1,*], Anna Bogdanova[1,*], Yerkebulan Nartbay [1]

[1] Abylkas Saginov Karaganda Technical University,
Nazarbayev Ave., No. 56, Karaganda 100027, Kazakhstan;
zhalelaigerim@mail.ru, a.dostayeva@ktu.edu.kz, aneta.2011@mail.ru, e.nartbay@ktu.edu.kz
* Correspondence: aneta.2011@mail.ru, a.dostayeva@ktu.edu.kz

Abstract

This study investigates the effect of complex alloying on the microstructure and mechanical behavior of modified 40H structural steel intended for metallurgical furnace rollers. The steel was modified with Ni, Mo, Al, and FeCrAl-based additives and subjected to normalization at 880°C, quenching at 860°C, and tempering at 550°C. Microstructural evolution was analyzed by scanning electron microscopy (SEM) with EDS characterization, while hardness was evaluated using Rockwell (HRC), Brinell (HBW), and Vickers (HV) methods.

The as-cast condition exhibited a heterogeneous cast microstructure characterized by pronounced dendritic segregation and significant hardness scatter (473–561 HB). After heat treatment, the microstructure developed a more uniform and refined appearance, accompanied by a reduction in hardness scatter. Hardness values stabilized in the range of 42-48 HRC, accompanied by a decrease in measurement dispersion. SEM/BSE observations indicated a more uniform morphology after heat treatment, while local SEM/EDS analysis was used only as a supplementary semi-quantitative tool to evaluate elemental distribution in selected regions.

The combined alloying and heat-treatment strategy contributed to microstructural refinement and reduced hardness scatter after heat treatment. These findings suggest that the proposed processing route may be beneficial for the development of 40H steel components intended for furnace roller applications.

Keywords: 40H steel; complex alloying; Ni-Mo modification; FeCrAl; heat treatment; SEM/BSE analysis; local EDS assessment; furnace roller applications

Academic Editor(s): Name

Received: date
Revised: date
Accepted: date
Published: date

Citation: Zhalel, A.; Issagulov, A.; Dostayeva, A. Development and Microstructural Investigation of Ni–Mo–FeCrAl Modified 40H Steel for Furnace Roller Applications. *Alloys* **2026**, *4*, x. https://doi.org/10.3390/xxxxx

Copyright: © 2025 by the author. Licensee MDPI, Basel, Switzerland. This article is an open access article distributed under the terms and conditions of the Creative Commons Attribution (CC BY) license (https://creativecommons.org/licenses/by/4.0/).

1. Introduction

Metallurgical furnaces used in various metallurgical processes, such as smelting, annealing, roasting, rolling, and heat treatment, operate under extremely high temperatures and significant mechanical and chemical stress. Reliability and longevity of these units directly depend on the quality of the materials and the processing technologies used. In this regard, one of the key components of metallurgical furnaces, the roller, is particularly important.

The roller is a crucial structural element of various furnace types that ensures their stable operation and process efficiency. They perform several key functions: they support

and move metal blanks, ingots, and products within the furnace facilitating their uniform heating or melting; they reduce friction between materials and furnace structural components, thereby reducing equipment wear; they operate in areas with extreme temperatures (up to 1000-2000°C), therefore they are made of high-strength and heat-resistant materials; they distribute mechanical loads reducing the impact on the other furnace components. Thus, a roller is an important component of metallurgical furnaces, the operational characteristics of which largely determine reliability and efficiency of the entire production process [1,2].

At high temperatures and intense exposure to aggressive gas environments, metallurgical furnace rollers are subject to significant thermal and mechanical loads. The key requirements for these components are high heat resistance, wear resistance, thermal fatigue resistance, and resistance to peeling. Alloyed structural steels, especially the 40H grade, are traditionally used for their production, since they offer good mechanical properties and processability. However, with prolonged operation at temperatures above 700-800°C, this steel loses strength which leads to deformation, cracking, and premature roller failure [3-5].

An effective way to improve the performance properties of steel is alloying and modifying the structure by introducing additional elements that form thermally stable phases. FeCrAl alloys are particularly promising, since they provide high heat resistance and the ability to form a dense Al_2O_3 oxide film on the surface, preventing further oxidation at elevated temperatures (typically above 800-1000°C). Under such conditions, conventional steels tend to form unstable oxide scales that can spall (flaking) during thermal cycling. The introduction of FeCrAl alloying can therefore improve thermal stability and reduce oxide scale spallation during high-temperature service [6].

The addition of a molybdenum (Mo) mixture positively affects heat resistance and strength properties of steels as it suppresses the granule growth and increases sliding resistance. It can be expected that the combined introduction of fechral and molybdenum into 40H steel will significantly improve its performance under high-temperature operating conditions [7-9].

In recent years, significant contributions to the development of heat-resistant and alloyed steels have been made by researchers from China, Japan, and South Korea. These studies focus on improving high-temperature oxidation resistance, microstructural stability, and mechanical performance through complex alloying strategies [10-12].

In particular, Fe-Cr-Al-based systems have attracted considerable attention due to their ability to form stable protective Al_2O_3 oxide films at elevated temperatures, which significantly enhances oxidation resistance [10,12,16]. Recent studies by Chinese researchers have demonstrated that FeCrAl alloys exhibit excellent high-temperature strength, corrosion resistance, and creep stability, making them promising candidates for extreme environments [11,14].

Furthermore, investigations conducted in South Korea have confirmed the formation of dense alumina oxide layers and their critical role in improving oxidation resistance under high-temperature steam conditions [12,17]. Additional studies have shown that alloying modifications and microalloying elements can further enhance oxidation resistance and structural stability by influencing oxide film formation mechanisms and diffusion processes [13-15].

Therefore, incorporating insights from these studies provides a strong scientific basis for the present work and supports the use of FeCrAl-based alloying systems for modifying 40H steel intended for furnace roller applications.

The purpose of this study is to improve the performance of metallurgical furnace rollers by modifying 40H steel with fechral and molybdenum additives.

To achieve this purpose, the following research objectives were addressed:

- melting 40H steel with varying amounts of fechral and molybdenum;

- studying the effect of alloying additions on the microstructure and local elemental distribution of the steel;

- determining changes in mechanical properties (hardness, strength, impact resistance) compared to the original steel;

- evaluating the microstructural characteristics and hardness behavior of the modified steel after alloying and heat treatment;

- substantiating the optimal composition and process parameters for modification based on the data obtained.

2. Methods

The base material used in this study was 40H structural steel. Its nominal chemical composition is presented in Table 1, and the corresponding critical transformation temperatures are listed in Table 2. Owing to its favorable combination of strength and manufacturability, this steel is widely used for high-temperature components. The aim of the experiment was to investigate the effect of FeCrAl and molybdenum alloying on the microstructure and properties of steel intended for furnace roller production.

Table 1. The chemical composition of 40H steel (%) was as follows.

C	Si	Mn	Ni	S	P	Cr	Cu
0.36-0.44	0.17-0.37	0.5-0.8	to 0.3	to 0.035	to 0.035	0.8-1.1	to 0.3

Table 2. Critical transformation temperatures of 40H steel

Ac_1 = 743°C	$Ac_3(A_{cm})$ = 782°C	$Ar_3(Ar_{cm})$ = 730°C	Ar_1 = 693°C

The work began with the smelting of the base material, 40H steel. This steel is widely used in mechanical engineering due to its satisfactory combination of strength, wear resistance, and processability. However, its performance characteristics under prolonged exposure to high temperatures are limited and necessitate targeted alloying for use as furnace rollers.

Based on an analysis of scientific and technical literature and the operating requirements of furnace rollers (high temperatures, cyclic heating and cooling, oxidizing atmosphere, mechanical loads), a decision was made to modify the chemical composition of 40H steel by means of introducing a ferrochromium-aluminum alloy (fechral) and molybdenum.

This significantly reduces the intensity of high-temperature oxidation and scale formation during metallurgical furnace operation at temperatures up to 1000-1100°C. Furthermore, the presence of chromium and aluminum increases thermal stability of the structure and improves resistance to corrosion in gas environments.

The introduction of molybdenum is aimed at increasing heat resistance and creep resistance under long-term loads. Molybdenum promotes solid solution strengthening, increases recrystallization temperature, slows diffusion and grain growth processes during high-temperature operation, and increases resistance to temper embrittlement. Additionally, molybdenum improves resistance to thermal fatigue and cracking during cyclic heating and cooling.

The charge composition used for experimental melting of the modified 40H steel is presented in Table 3. The additions of FeCrAl, molybdenum, nickel, and aluminum were selected to improve oxidation resistance, structural stability, and high-temperature strength.

At the same time, the carbon values obtained by EDS should be interpreted with caution, since carbon is difficult to quantify reliably by this method due to its low char-

acteristic X-ray energy and the possible contribution from surface contamination or sample preparation media. Carbon values obtained by EDS are approximate and may be overestimated because of the limited accuracy of the method for light elements. The FeCrAl alloy used in this study had a typical industrial composition consisting of approximately 20-25 wt.% Cr, 4-6 wt.% Al, and the balance Fe.

Table 3. Charge composition used for the experimental melting of modified 40H steel

Component	Mass, g	Mass fraction in the charge, %
40H steel (base)	230.00	94.02
Fechral	1.92	0.79
Molybdenum	0.64	0.26
Nickel	10.60	4.33
Aluminum	0.33	0.13
Total	**243.49**	**100.00**

The composition presented in Table 3 was selected based on the need to achieve a balance between oxidation resistance, high-temperature strength, and structural stability. The addition of FeCrAl (~0.8 wt.%) promotes the formation of a protective oxide layer, significantly improving oxidation resistance. Molybdenum (~0.25 wt.%) enhances creep resistance and suppresses grain growth at elevated temperatures. Nickel (~4 wt.%) improves hardenability and toughness of the matrix. The selected composition represents an optimal compromise between performance improvement and technological feasibility, supported by literature data and preliminary experimental considerations.

Alloying elements were introduced in the form of small granules with a typical size of approximately 3-10 mm to ensure rapid melting and uniform distribution within the liquid metal.

Before melting, sand-resin shell molds were prepared for casting the experimental samples. The molds were manufactured using the variational static-pressure technology developed within project AP26103581, in which the pressure applied to the sand-resin mixture was sequentially changed from 0.23 MPa to 0.45 MPa and subsequently reduced to 0.17 MPa. The resulting shell molds, with a thickness of approximately 10–12 mm, were subsequently sintered at 330–350 °C for 100–120 s before metal pouring.

Melting was performed in an induction furnace. Melting was carried out under atmospheric conditions to simulate typical industrial processing environments. Compared to vacuum or argon melting, atmospheric melting is more economically feasible but may lead to increased oxidation and inclusion formation. However, the addition of FeCrAl contributes to the stabilization of oxide phases and partially compensates for these effects. First, the base material, 40H steel, was placed in a crucible. After reaching the temperature of approximately 1500°C, alloying elements were gradually added to the melt according to the design scheme. The melting temperature of the alloying system was estimated based on phase diagrams and literature data and remained within the operational range of the induction furnace (~1500°C). This temperature ensured complete melting of all components and sufficient homogenization of the liquid metal.

After melting, the metal was poured into pre-prepared sand-resin shell molds. Cooling was carried out at the room temperature. Air cooling was selected to replicate realistic casting conditions. More rapid cooling media such as water or oil can significantly alter phase transformation kinetics, leading to increased residual stresses and potential distortion. The influence of different cooling media on the microstructure and

properties of the alloy will be investigated in future work. Thus, the alloying process took place directly in the furnace which ensured a uniform chemical composition and a stable modification process. After melting, the metal was poured into pre-prepared and heated sand molds. The resulting cast sample is presented in Figure 1.

The resulting samples were subsequently studied, including chemical composition determination, metallographic structural analysis, and mechanical property measurements.



Figure 1. A sample after melting in the molding furnace.

After the sample had completely cooled and hardened, the next stage began: surface smoothing. Grinding was performed in the KORMS laboratory at Karaganda Technical University. A Labopol/Laboforce grinding and polishing machine was used for grinding. Since the studied material was 40H steel, a suitable grinding method was selected.

The method selected for this machine depends on the type of material.

Table 4. Selected machining method for 40H steel

Step	Smoothing	Fine grinding (FG)	Diamond polishing (DP)
Disc type	MD-Piano 220	MD-Allergo	MD-Dac
Suspension type	Water	Diamond suspension 9 μm	Diamond suspension 3 μm
Lubricant	-	green/blue	green/blue
Rotation speed (rpm)	300	150	150
Force	240	180	180
Preparation time (min)	Before smoothing	4	4

The MD-Piano 220 disc was used for the initial grinding stage. The surface was wetted with water, and the rotation speed was set to 300 rpm. Grinding was continued until a smooth and uniform surface was obtained. The relatively long grinding time (approximately 1-1.5 h) was due to the small size of the specimens, manual sample handling, and the need to remove the as-cast surface layer containing roughness and possible casting-related defects.

For the second stage, the MD-Allergo disc was selected. The specimen was rinsed with water between processing stages. A 9-μm diamond suspension was used at this stage. The rotation speed was reduced to 150 rpm, and a lubricant was additionally applied. The processing time was approximately 30 minutes.

For the final stage, the MD-Dac disc was installed. The specimen was rinsed again, after which a 3-μm diamond suspension was applied. Lubricant was applied several

times during processing. This resulted in specimens with a smooth surface, ready for further analysis.

After obtaining the sample with a smooth surface, it was treated with the 3-4% HNO_3 solution for etching. The etching revealed the material microstructure and more clearly defined its phase components. The goal of this stage was to obtain reliable and illustrative structural analysis results.

Hardness measurements were performed using Rockwell (HRC), Brinell (HBW), and Vickers (HV) methods in accordance with standard testing procedures (ISO standards). The applied loads and dwell times were selected to ensure reliable and reproducible results. Multiple measurements were carried out on each sample, and the average values were used for analysis.

Microstructural analysis was performed using a JEOL JCM-7000 (NEOSCOPE) scanning electron microscope. The samples were placed in a dedicated chamber and analyzed under controlled conditions using appropriate software. The analysis focused on evaluating microstructural morphology, contrast variations, and structural heterogeneity.

EDS analysis was used only for local semi-quantitative assessment of elemental distribution in selected regions. It was not used to determine the bulk chemical composition of the alloy or to identify phases definitively. Therefore, all EDS results presented in this work should be interpreted as qualitative or semi-quantitative observations of local elemental distribution.

3. Results

According to scanning electron microscopy data obtained in backscattered electron mode (BED-S), the image contrast is determined by the difference in the average atomic numbers of the phases: the higher the average atomic number, the lighter the region in the micrograph.

Figure 2 (×400, scale factor 50 μm) shows pronounced structural heterogeneity. The light gray areas form the main metallic matrix. Given the alloy composition, the matrix likely consists of an alloyed iron base with dissolved nickel and, to some extent, molybdenum.

Dark features observed in the BSE images were interpreted either as pores or as non-metallic inclusions based on morphology and EDS response. Pores appear as very dark void-like regions without measurable elemental signal, whereas inclusions show compositional contrast and detectable enrichment in elements such as Al, Si, and O. Therefore, the pinpoint dark features discussed here are attributed to oxide inclusions rather than porosity. Given the presence of aluminum and FeCrAl components, these features may correspond to non-metallic inclusions; however, their exact composition cannot be conclusively determined from the available observations.

Individual brighter areas may be associated with localized compositional variations related to alloying additions; however, their exact nature cannot be conclusively determined from the present observations.

The overall structure exhibits an acicular or lamellar morphology resulting from crystallization and subsequent cooling. As shown in Figure 2a, the as-cast modified 40H steel exhibits a heterogeneous dendritic microstructure. Figure 2b reveals local structural defects and dark dispersed features. Higher magnification (Figure 2c) shows fine dark particles, which are interpreted as non-metallic inclusions.

The light gray areas correspond to the metallic matrix enriched with heavier elements. Brighter regions are observed in areas with a higher average atomic number, while darker regions are associated with phases containing elements of lower atomic number.

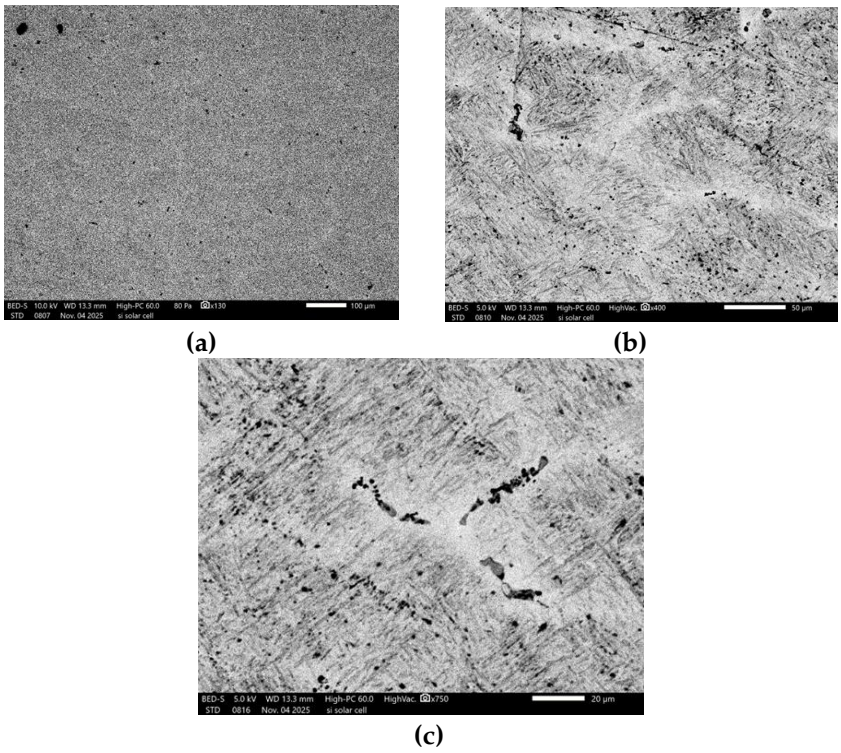


Figure 2. SEM micrographs of the as-cast modified 40H steel: (a) overview image showing the heterogeneous dendritic microstructure; (b) higher-magnification image showing local dark dispersed features and structural heterogeneity; (c) high-magnification image showing fine dark particles interpreted as non-metallic inclusions.

The following defects were identified in the studied microstructure:

- randomly directed microcracks and micropores;
- localized structural zones of heterogeneity.

The microstructure is characterized by the presence of micropores with sizes ranging from 1 to 5 μm. These pores are irregular in shape and unevenly distributed throughout the material, with most of them being isolated rather than interconnected.

Backscattered electron (BSE) analysis revealed a finely dispersed and heterogeneous microstructure. The metallic matrix appears as light-gray regions, while darker areas correspond to local features exhibiting lower BSE contrast. The structure also contains microcracks with sizes up to 5 μm, which are attributed to thermal stresses arising during cooling.

Overall, the microstructure exhibits localized heterogeneities within a relatively uniform matrix appearance.

To eliminate the identified structural defects (microcracks, localized inhomogeneities, and residual porosity) and to improve heat resistance and mechanical properties, a comprehensive heat treatment was applied. This treatment aimed to produce a more uniform microstructure, reduce internal stresses, decrease structural heterogeneity, and improve overall structural uniformity [18–26].

The heat treatment was performed in a muffle furnace and included three sequential stages. The first stage involved normalization at 880°C, a 2-hour hold, and subsequent air cooling. This mode helped to equalize chemical and structural inhomogeneities, refine the grain size, and reduce residual stresses after casting. The detailed heat treatment schedule is presented in Figure 3.

The second stage consisted of austenitization at 860°C with a holding time of 40 min, followed by cooling in air to room temperature. This treatment promoted the formation of a hardened microstructure and contributed to improved hardness and wear resistance.

The final stage involved medium tempering at 550°C for 2 hours, followed by air cooling. Tempering reduced internal stresses and contributed to microstructural stabilization.

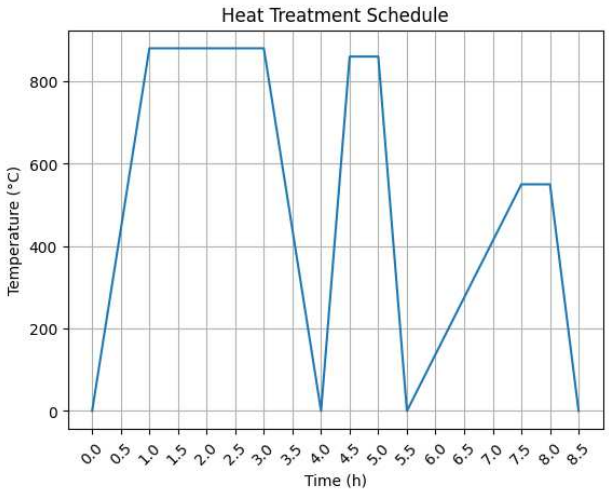


Figure 3. Heat treatment schedule of modified 40H steel, including normalization, quenching, and tempering stages

After medium tempering, the steel developed a more stable microstructural appearance with reduced hardness scatter and improved structural uniformity. The applied heat-treatment schedule contributed to stress relaxation and stabilization of the mechanical response of the material. To evaluate the effectiveness of heat treatment, comparative microstructural analysis was performed before and after processing.

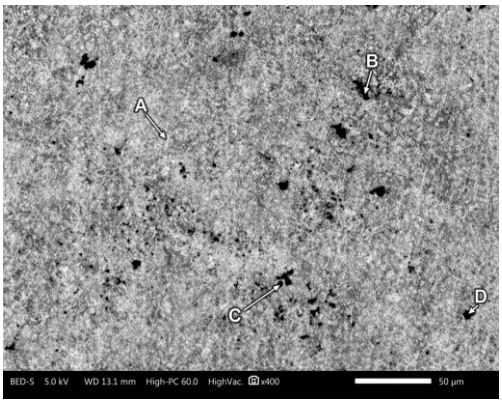


Figure 4. SEM/BSE micrograph of modified 40H steel after heat treatment, showing a refined matrix morphology with local dark dispersed features. The marked regions indicate: A — representative matrix region; B — dark dispersed feature; C — cluster of dark features; D — isolated dark particle. The exact chemical nature of these features cannot be definitively determined from SEM/BSE observation alone.

As shown in Figure 4, the microstructure after heat treatment exhibits a relatively uniform BSE contrast and a refined appearance compared with the as-cast condition. Region A represents the metallic matrix, while regions B–D highlight local dark features observed within the examined area. The origin and composition of these features cannot be conclusively determined based on the present SEM/BSE observations alone and require additional analytical techniques for confirmation. A comparative summary of the structural characteristics of the modified 40H steel before and after heat treatment is presented in Table 5.

Table 5. Comparison of structural characteristics before and after heat treatment

Comparison parameter	Melted state	After heat treatment
Microstructure type	Heterogeneous cast structure with pronounced dendritic morphology	Refined and more homogeneous matrix morphology.
Basic phase composition	Heterogeneous cast microstructure with acicular and dendritic features	Refined microstructure after heat treatment
Phase morphology	Large acicular formations surrounded by a dendritic network	Refined matrix with dispersed dark features.
Grain size/structural scale	Coarse and heterogeneous microstructure	More uniform and refined microstructural appearance
Elemental distribution	Local compositional heterogeneity associated with solidification	Local elemental distribution requires further confirmation by mapping.
Internal stresses	High residual stresses after solidification	Reduced due to normalization and tempering.
Mechanical properties	Higher hardness scatter and greater structural heterogeneity	More stable hardness values and reduced scatter.

Before processing, the steel exhibits a coarse and heterogeneous structure.

After processing, the microstructure exhibits a more refined and uniform appearance compared with the as-cast condition. The applied heat-treatment schedule contributed to the reduction of structural heterogeneity and residual stresses.

After heat treatment, the microstructure of the modified 40H steel exhibits a more uniform appearance and reduced structural heterogeneity compared with the as-cast condition. This transformation is accompanied by a reduction in structural heterogeneity and improved structural uniformity.

As a result, hardness values decrease slightly compared to the as-cast condition but become more stable and uniform across the sample, reaching a range of 42-48 HRC (390–450 HB). In contrast to the initial state, which is characterized by significant hardness scatter (473-561 HB) due to dendritic segregation and residual stresses, the heat-treated material exhibits a more consistent and reliable mechanical response.

The resulting microstructural condition is associated with more stable hardness values and reduced measurement scatter compared with the as-cast state.

The hardness data for the as-cast state show relatively high average values for the modified 40H steel (52.0 ± 2.3 HRC, 498.2 ± 5.9 HBW, and 452.8 ± 0.8 HV). These results indicate the influence of alloying additions on the formation of a hardened microstructure during solidification and cooling.

However, the as-cast condition exhibits greater hardness scatter, indicating a higher degree of structural heterogeneity.

After normalization, quenching, and medium tempering (at 550°C), the hardness decreased compared with the as-cast condition but became more stable and uniform throughout the material. For furnace roller applications, stable hardness values are considered important for reliable service performance.

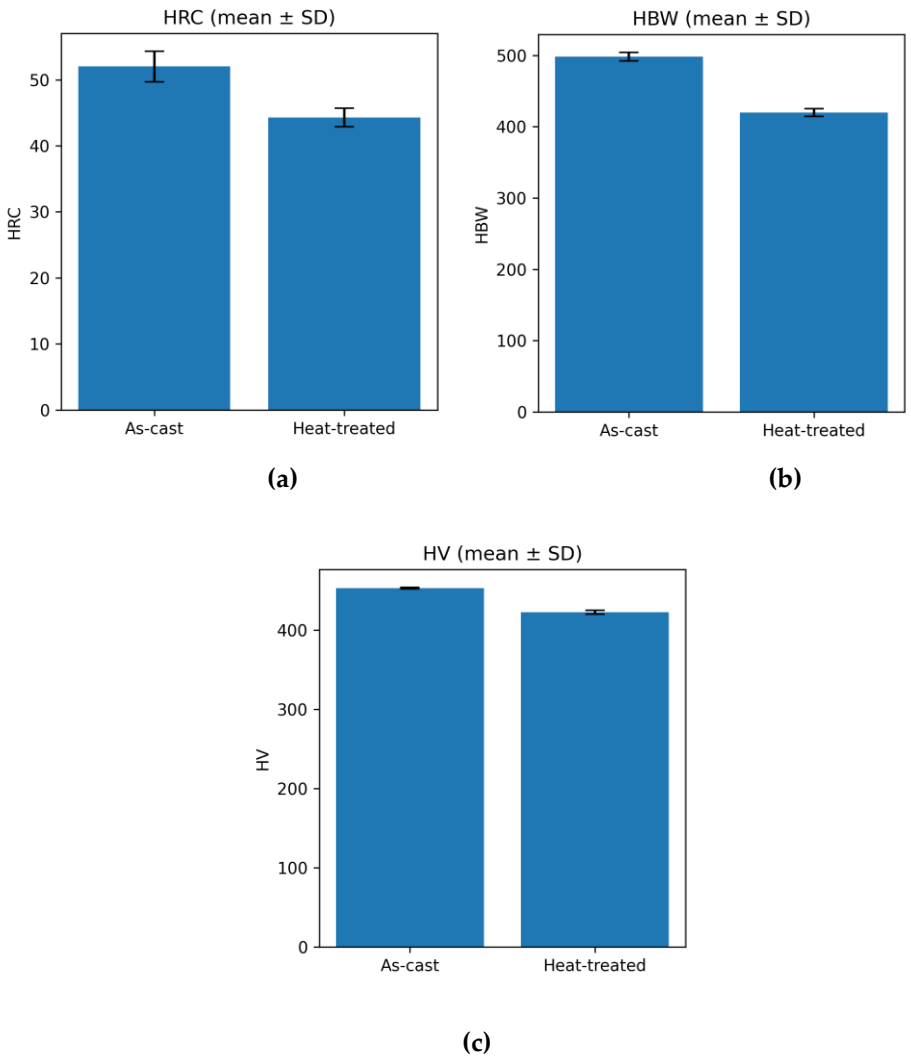


Figure 5. Average hardness values of modified 40H steel before and after heat treatment measured by (a) Rockwell hardness (HRC), (b) Brinell hardness (HBW), and (c) Vickers hardness (HV). Error bars represent the standard deviation of five independent measurements.

The optimal hardness, ensuring improved steel quality in this condition, is 40-48 HRC (or approximately 380-450 HB/HV). This hardness range is consistent with the development of a more stable microstructural condition after heat treatment and provides a favorable balance between hardness and structural uniformity. At the same time, the working roller maintains sufficient hardness for effective wear resistance, but at the same time it does not become excessively brittle, which is favorable for maintaining structural stability during service. As shown in Figure 5, the hardness values are presented as mean values with standard deviation calculated from five independent measurements. The as-cast steel exhibited higher hardness values but also a greater measurement scatter. After heat treatment, the average hardness decreased to 44.3 ± 1.4 HRC, 420.0 ± 5.4 HBW, and 422.4 ± 2.3 HV, indicating stress relaxation and microstructural stabilization. The relatively small standard deviations after heat treatment suggest improved structural uniformity and more consistent mechanical properties throughout the material. Overall, the heat-treated material demonstrates reduced scatter and more uniform hardness values compared to the as-cast state.

4. Discussion

SEM/BSE observations revealed a more uniform matrix morphology after heat treatment compared with the as-cast condition. Dark dispersed features were observed

throughout the microstructure, while the overall contrast distribution appeared more homogeneous. The available EDS measurements were used only as a local semi-quantitative assessment of elemental distribution and were not intended for bulk chemical composition determination or definitive phase identification.

The SEM observations suggest that heat treatment contributed to the reduction of structural heterogeneity and the development of a more uniform microstructural appearance. However, the exact nature of the observed dark features cannot be conclusively determined without additional analytical techniques such as elemental mapping, X-ray diffraction, or other phase-identification methods.

Although SEM/EDS analysis provides valuable information on the elemental distribution and microstructural features, it does not allow for definitive phase identification. Therefore, additional phase analysis using X-ray diffraction (XRD) is required to confirm the presence of specific phases such as carbides and intermetallic compounds. The present study focuses on microstructural characterization, however, comprehensive phase identification will be addressed in future work.

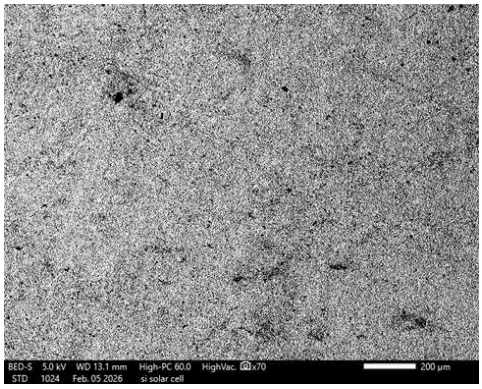


Figure 6. BSE micrograph (×70) of modified 40H steel after heat treatment, showing the overall morphology of the heat-treated steel and contrast variations observed in the BSE image.

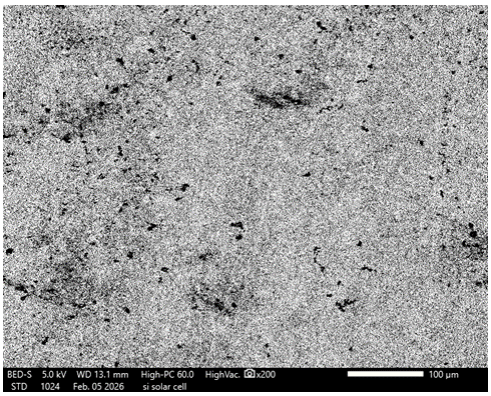


Figure 7. BSE micrograph (×200) of modified 40H steel after heat treatment, showing a refined matrix morphology with dispersed dark features after heat treatment.

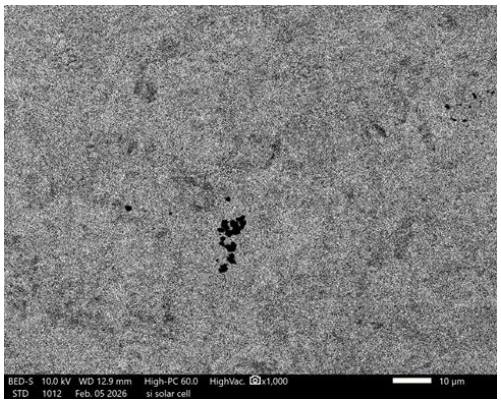


Figure 8. BSE micrograph (×1000) of modified 40H steel after heat treatment, showing local dark dispersed features and contrast heterogeneity within the metallic matrix.

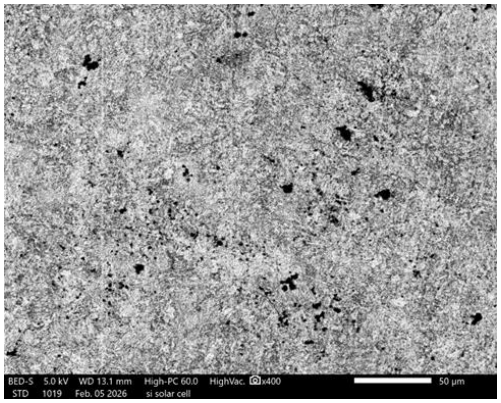


Figure 9. BSE micrograph (×400) of modified 40H steel after heat treatment, showing the spatial distribution of dispersed dark features within the metallic matrix.

As shown in Figure 6, the heat-treated modified 40H steel exhibits a relatively uniform matrix contrast in the BSE image. Dark dispersed features are observed throughout the microstructure; however, their exact composition and phase nature cannot be conclusively determined from the present observations alone. No obvious macrosegregation or large-scale structural defects are observed within the examined field of view. A relatively uniform matrix contrast is visible in the BSE image.

A higher magnification image (Figure 7) reveals a refined matrix morphology with local contrast variations and dispersed dark features. The observed morphology is consistent with the microstructural changes expected after heat treatment; however, definitive phase identification requires complementary analytical techniques.

High-magnification analysis (×1000), presented in Figure 8, reveals fine clusters of dark features and local heterogeneities. The dark regions appear as compact agglomerates in the micrometer range; however, their exact nature cannot be conclusively determined from the present observations and requires additional analytical confirmation. The surrounding matrix exhibits a refined appearance.

As shown in Figure 9 (×400), dispersed inclusions are irregularly distributed within the metallic matrix but do not form continuous networks, which is favorable for mechanical integrity. The absence of large elongated defects or continuous feature networks suggests a relatively uniform microstructural appearance.

Overall, the SEM observations and hardness measurements indicate that complex alloying of 40H steel with Ni, Mo, and FeCrAl, followed by normalization, quenching, and tempering, contributed to a more uniform microstructural appearance and improved hardness stability. SEM analysis revealed a transition from a heterogeneous cast structure

to a refined morphology with dispersed dark features and a more uniform contrast distribution. The reduction and stabilization of hardness after heat treatment suggest a decrease in structural heterogeneity and residual stresses. The obtained results demonstrate the positive effect of the proposed alloying and heat-treatment strategy on the microstructural condition and mechanical response of the modified steel. Future work will include elemental mapping, phase characterization by XRD, oxidation testing, and creep resistance evaluation.

5. Conclusions

The present study investigated the effect of complex alloying of 40H steel with Ni, Mo, Al, and FeCrAl, combined with normalization, quenching, and tempering, on the microstructural characteristics and hardness behavior of the alloy. SEM observations revealed a transition from a heterogeneous cast structure to a more refined and uniform microstructural appearance after heat treatment.

The hardness measurements demonstrated a reduction and stabilization of hardness values after heat treatment, from 473–561 HB in the as-cast condition to a stable range of 42–48 HRC. The decreased hardness scatter indicates improved structural uniformity and reduced residual stresses within the material.

The combination of alloying and heat treatment resulted in a refined microstructural morphology and more consistent mechanical response compared with the initial cast condition. These results suggest that the proposed processing route is a promising approach for improving the performance characteristics of 40H steel intended for furnace roller applications.

The obtained findings provide a basis for future investigations involving detailed phase characterization, elemental mapping, oxidation resistance evaluation, and high-temperature performance testing.

Author Contributions: Conceptualization: A.D., Methodology: A.Zh., Y.N.; Formal Analysis: A.D.; Investigation A.Zh.; Writing—Original Draft Preparation: A.Zh., A.B. and A.D. Funding Acquisition: A.I. All authors have read and agreed to the published version of the manuscript.

Funding: These studies were carried out within the framework of the grant of the Committee of Science of the Ministry of Internal Affairs of the Republic of Kazakhstan AP26103581 “Development and research of a cost-effective technology for producing precision castings in sand-resin molds obtained using variational static pressure”.

Data Availability Statement: All data generated or analysed during this study are included in this published article.

Conflicts of Interest: The authors declare no conflicts of interest.

References

1. Jaromin, M.; Dojka, R.; Jezierski, J.; Dojka, M. Influence of Type and Shape of the Chillon Solidification Process of Steel Casting. Arch. Foundry Eng. 2019, 19, 35–40.
2. M. Bašistová, F. Radkovský, P.Lichý, Š. Kielar and I. Vasková Numerical Simulation and Optimization of Furnace Roll Casting Production Technology. Materials 2025, 18(23), 5445; https://doi.org/10.3390/ma18235445
3. R. Erica Gordon, E. Eric Kalu, A. Rasak Adetunji, D. Campbell, P. N. Kalu The Effect of the Environment on the Case Hardening Characteristics of AISI 1018 Steel during Cassava Leaf Pack Cyaniding Alloys2024, 3(1), 1-14; https://doi.org/10.3390/alloys3010001
4. Irakli Nakhutsrishvili, Revaz Tevzadze. Oxidation Kinetics of FeCr and FeCrAl Alloys: Influence of Secondary Processes (Continuation) Alloys 2025, 4(1), 2; https://doi.org/10.3390/alloys4010002
5. Issagulov A.Z., Kvon S.S. and Kulikov V.Yu. Increasing the wear resistance of 30H3MF steel by additional alloying. Proceedings of the XXIII International Scientific and Production Conference "Innovative Solutions in Agricultural Science - a Look into the Future" (May 28-29, 2019). Maisky, Russia, pp. 80-82.
6. Goldstein M.N., Grachev S.V. and Veksler Yu.G. Special steels. M, Metallurgy, 1989

7. Perelygin V. Hardox: Let's sort it out calmly. Fixed Assets, 2008. No. 12
8. New high-strength weldable wear-resistant steel with a tensile strength of at least 1050 N/mm2. Metallurgist, 2005, No. 1, pp. 51-54.
9. H. Duzcukohfu. Effect of boron addition on Mechanical properties of 60SiCr7Steel. Int. J.of Materials, Mechanic and Manufactory. 2015. V. 3. No. 2, 2015
10. Li, Z.; H. Duzcukohfu. Effect of boron addition on Mechanical properties of 60SiCr7Steel. Int. J.of Materials, Mechanic and Manufactory. 2015. V. 3. No. 2, 2015Chen, L.; Zhang, H.; Liu, S. High-Temperature Oxidation Properties and Microstructural Evolution of Nanostructure Fe-Cr-Al ODS Alloys. Materials 2021, 14(3), 526. https://doi.org/10.3390/ma14030526.
11. Gao, Z.; Wang, X.; Zhou, D.; Wu, Q.; Li, C.; Song, L.; Liu, S. The Formation Mechanism of a Multilayer-Structure Oxide Film during the Oxidation of FeCrAl in Air at 700 °C. Metals 2023, 13(2), 305. https://doi.org/10.3390/met13020305.
12. Chikhalikar, A.; Roy, I.; Abouelella, H.; et al. Effect of Aluminum on the FeCr(Al) Alloy Oxidation Resistance in Steam Environment at Low and High Temperatures. Corrosion Science 2022, 209, 110765. https://doi.org/10.1016/j.corsci.2022.110765.
13. Wu, Z.; Wen, G.; Han, Y. Grain Growth and Oxidation Resistance of Fe–Cr–Al Electrothermal Alloy Doped with Yttrium. Advances in Materials Science and Engineering 2020, 29–36. https://doi.org/10.18280/acsm.440104.
14. Zhang, X.; et al. High-Temperature Oxidation of Oxide-Dispersion-Strengthened FeCrAl Alloys: Influence of Alloying Elements. Journal of Materials Research and Technology 2024, 30, 9196–9204. https://doi.org/10.1016/j.jmrt.2024.06.011.
15. Liu, Y.; et al. Microstructure Evolution and Oxidation Resistance of FeCrAl Alloys at Elevated Temperatures. Vacuum 2024, 227, 113371. https://doi.org/10.1016/j.vacuum.2024.113371.
16. Engkvist, J.; Bexell, U.; Grehk, M.; Olsson, M. High-Temperature Oxidation of FeCrAl Alloys—Influence of Al Concentration on Oxide Layer Characteristics. Materials and Corrosion 2009, 60(11), 876–881. https://doi.org/10.1002/maco.200805186.
17. Hellström, K.; Israelsson, N.; Mortazavi, N.; Canovic, S.; Halvarsson, M.; Johansson, L.-G. Oxidation of a Dispersion-Strengthened FeCrAl Alloy in the Presence of Oxygen at 1100°C. Oxidation of Metals 2015, 83, 533–558. https://doi.org/10.1007/s11085-015-9534-7.
18. A. Gottwalt-Baruth, P. Kubaschinski, M. Waltz and U. Tetzlaff. Influence of Subsequent Heat Treatment on Fatigue Behavior of Shear-Cut Electrical Steel Sheets. Alloys2024, 3(4), 281-294; https://doi.org/10.3390/alloys3040017.
19. Toleuova, A.R., Dostayeva, A.M., Zharkevich, O.M. and Adilkanovva, M.A. (2020). Calculating and experimental studying phase transformations in the Al-Zr-Fe-Si system alloys, Metalurgija, 59(4), pp. 543–546
20. Kulikov, V.Y., Aubakirov, D.R., Kvon, S.S. et al. Use of Wear-Resistant Materials in the Kazakhstani Metallurgical Industry. Metallurgist 62, 1068–1072 (2019). https://doi.org/10.1007/s11015-019-00755-5
21. Belov N.A., Korotkova N.O., Dostayeva A., Akopyan T.K. (2015). Influence of thermomechanical treatment on electrical resistivity and hardening of alloys Al - 0.2 % Zr and Al - 0.4 % Zr. Tsvetnye Metally, 10, pp. 13–18
22. Kovalyova, T., Yeremin, E., Arinova, S., Medvedeva, I. and Dostayeva, A. (2017). Enhancing surface roughness of castings when sand-resin mold casting. Metalurgija, 56(1-2), pp. 135–138
23. A. Dostayeva, A. Issagulov, M. Abdrakhmanov, A. Zhalel, A. Toleuova Integrated ladle treatment of 40HN3MF steel using fesial and femn for metallurgical rollers D.Serikbayev EKTU Bulletin, 2026, 1, 1-13
24. Orlov V.V., Malyshevsky V.A., Khlusova E.A. and Golosienko S.A. Development of technology for the production of structural steels for marine equipment and main pipelines intended for operation in the Arctic, Steel, 2014, No. 9, pp. 79-88.
25. Gulyaev A.P. Metal Science. Publisher: M.: Metallurgy, 2001
26. Likholobov E.Yu. Improving the quality of high-manganese steel castings by improving the process of its melting and out-of-furnace treatment. M., 2012. P. 3-4.

Disclaimer/Publisher's Note: The statements, opinions and data contained in all publications are solely those of the individual author(s) and contributor(s) and not of MDPI and/or the editor(s). MDPI and/or the editor(s) disclaim responsibility for any injury to people or property resulting from any ideas, methods, instructions or products referred to in the content.